Laser cladding and wear testing of nickel base hardfacing materials influence of process parameters

P. Aubry, C. Blanc, I. Demirci, M. Dal, T. Malot, H. Maskrot

LASER CLADDING AND WEAR TESTING OF NICKEL BASE HARDFACING MATERIALS: INFLUENCE OF PROCESS PARAMETERS

Paper #303

P.Aubry[1], C.Blanc[1], I.Demirci[2], M.Dal[3], T.Malot[3], H. Maskrot[1]

1 Den – Service d'Etudes Analytiques et de Réactivité des Surfaces (SEARS), CEA, Université Paris-Saclay, F-91191, Gif-sur-Yvette, France
2 MPSM, Ecole Nationale Supérieure d'Arts et Métiers, Châlons-en-Champagne 5006, France
3 PIMM, Ecole Nationale Supérieure d'Arts et Métiers, Paris 75013, France

Abstract/Manuscript

In fast neutron reactors, some parts can be submitted to displacements between each other (as movable parts for example). On these parts, the contact areas usually need a hardfacing coating. The standard hardfacing alloy is a cobalt-base alloy (as, for example Stellite®6). Unfortunately, in the primary coolant circuit and on wear conditions, cobalt can be released. Under neutron flux, the ^{59}Co, stable, can be transmuted into ^{60}Co by radioactive capture of neutrons and, therefore, can contaminate the primary circuit. Therefore, it is desired to replace this cobalt based hardfacing alloy by a cobalt-free one.

Previous presentations have shown the potential interest of some nickel base materials as Colmonoy® alloy (Colmonoy® 52 for laser cladding). In parallel, laser cladding has been identified as a deposition process that could increase the performances of the hardfacing materials compared to the standard process (Plasma Transferred Arc Welding). In all the study, the base material is the stainless steel 316LN.

In the article, we sump up the previous results related to the investigations on these alloys. Then, another alloy is presented: the Tribaloy® 700 is evaluated. This nickel base has a complete different microstructure and its tribological behavior related to the variation of the microstructure is not well known.

First, we present the selected materials. Then, we present the process parameter search. The quality of the clad is considered and the process window providing a good clad is determined (no crack, only few porosities,…). The variation of the microstructure is analyzed and solidification paths are proposed regarding the process parameters.

In parallel, a model of the laser cladding process is discussed and implemented under COMSOL® software. Finally a simulation is presented and compared to the real clad.

Finally, wear tests are performed on typical wear conditions. The movement is linear. Argon is used for protection of the sample against oxidation. Tests are made at 200°C. Wear tests are analyzed and wear mechanisms are correlated to the microstructure of the material.

Introduction

The main feature of Fast Neutron Reactors in the field of tribology is due to the use of an alkali metal as a coolant such as liquid sodium. The liquid sodium has the ability to reduce many metal oxides. This avidity depends on the nature of the oxides, and the temperature. For reasons related on one hand to the risk of clogging of pipes and on the other hand to corrosion and transfer of activation products, it is necessary to purify the primary and secondary sodium by passing it through cold traps. Thus, a lower temperature is maintained during operation for sealing as the impurity concentration (oxygen and hydrogen) is in the sodium lower itself. This purification increases the capacity of oxidation-reduction of sodium in particular against the oxides present on the surface of materials and whose influence on the friction is generally favorable. Similarly, the more the purification is pushed towards the low concentrations of oxygen, the less the formation of self-lubricant mixed oxides such as chromite or sodium aluminate is probable. Therefore, the minimum concentration of oxygen in the sodium is fundamental for tribology.

The first hardfacing materials used to overcome the problems of friction in sodium are cobalt based alloys, commonly used in several industrial fields. However, one major drawback of these alloys for nuclear applications is the activation of Cobalt under neutron flux in a reaction $^{59}Co\ (n, \gamma) \rightarrow {}^{60}Co$. With a period of 5.7 years, the activity of Cobalt 60 is maximum during operation of the reactor. A period of at least 30 years after the shutdown is necessary to observe a significant reduction of induced activity.

Thus, it is desirable to avoid these alloys for severe neutron flow and different studies tried to find substitute material without cobalt or in very small quantities.

There are different areas in SFR that have been identified as being most affected by friction (wear) as the strongback support on the primary vessel, candles assembly components, steam generator components, moving parts in valves…

The requirements are very demanding: tribo-corrosion under sodium, operating temperature from 180 to 500°C, risk of thermal shock and thermal cycling, and life spam of over 60 years without binding or degradation.

Selection of materials

The context of the future reactor implies a number of constraints on the possible choice of harfacing materials. Particularly, the range of the temperature between 200°C and 500°C during operation is very constraining for the selection of hardfacing alloys. First, it has been decided to keep on study Stellite 6 alloy, a cobalt-based material, as a reference.

Stellite® alloys

Stellite is the well know and widely used hardfacing wear resistance material. The Stellite alloy, from Deloro Company, is a cobalt-chromium base specially designed for abrasion resistance. There are many alloys of Stellite composed of variable proportions of cobalt, nickel, iron, aluminum, boron, carbon, chromium, manganese, molybdenum, phosphorus, sulfur, silicon and titanium, most alloys having four to six of these elements.

Stellite alloys have a high melting point and high hardness (eg Stellite 6: 40 HRC, melting point 1260°C-1357°C). They are therefore very difficult to machine. The hardness is strongly dependent on microstructure. The ductility of Stellite is mainly determined by the volume fraction of carbides and their morphologies. An increase of carbides reduces ductility. Under conditions of oxidation, the elements Cr and Co can form chromium and cobalt oxides at different oxidation levels (see P.M. Dunckley (1976) [1] and H. So (1996) [2]. The abrasion resistance is proportional to the hardness and increases with the proportion and size of carbides (see J.T.M de Hosson (1997) [3] and de Mol van Otterloo (1997) [4]).

A large number of Stellite substitutes has been proposed in the literature. Considering requirements, thick coatings are preferably retained. Among them, we can consider two main types of materials: the iron or nickel based alloys.If iron base alloys cannot be definitely excluded, the bibliography (D.H.E. Persson (2003) [5,6] and C. B. Bahn, (2004) [7]) mainly demonstrates the poor behavior of the iron-based hardfacing coatings at high temperature regardless of the deposition process.

At the opposite, authors have evidenced the interest of using Nickel based alloys for replacing the Cobalt based ones (see M. Corchia (1987) [8], Kashani (2007) [9]). Because of that, we have selected two promising nickel base alloys: Colmonoy® and Tribaloy®.

Colmonoy® alloys

The Colmonoy® is a nickel-based alloy developed by Wallcolmonoy Company which comprises hardening chromium borides and carbides. Its main interest is to be Cobalt free while providing different grades adapted to different wear and corrosion conditions. Colmonoy alloy has been investigated and the work is ongoing. Previous articles present results on laser cladding of Colmonoy 52 [10],[11],[12][13],

If the Colmonoy 52 is still under study, previous results has demonstrated the difficulty of obtaining crack free deposits with high energy processes as Plasma Transferred Arc Welding (PTAW) or laser cladding, the two processes selected in the research project.

Tribaloy® alloys

Tribaloy® alloys have been developed by the Deloro company. Grades are offered in nickel or cobalt base. They are particularly useful in the case of dried metal-metal tribo-corrosion at high temperature (800°C-1000°C). These grades have been developed to obtain a wear and corrosion behavior very close to Stellite. They may also contain a small proportion of cobalt.

The Tribaloy T-700 (see table 1 for composition) has a high resistance to corrosion and oxidation. It contains no cobalt and has been identified as a good candidate for nuclear applications. Note that its wear resistance is proportional to the volume fraction of the Laves phase present in the deposited material. Therefore, the results of wear tests are very sensitive to the process as dilution rate, cooling rate and overall thermal history of the clad.

The microstructure of the Tribaloy 700 coating comprises the Laves-phase whose volume is about

60% (see figure 1). Thanks to this phase, this coating has good wear resistance.

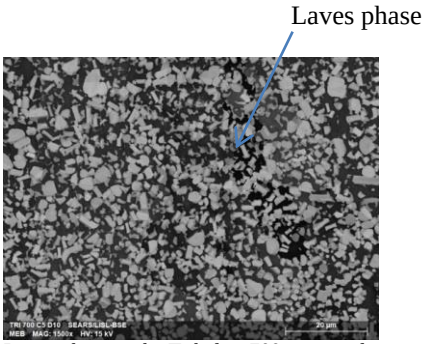

Figure 1 : Laves-phase in the Tribaloy-700 coating deposited by laser

The composition of the three materials (the Stellite is used as a reference) are presented in table

Chemical compisition	Materials (%weight)			
	AISI 316L	Stellite 6	Colmonoy 52	Tribaloy 700
B	-	-	2.2	-
C	0.02	0.9-1.4	0.55	<0.5
Co	-	Bal.	-	-
Cr	16-18	27-32	12.3	26
Fe	Bal.	-	3.8-4.8	<2.0
Mn	2-2.5	-	-	-
Mo	2	-	-	26
Ni	10.5-13.5	-	Bal.	Bal.
Si	1	-	3.7	<1.5
W	-	4-6	-	-

Table1: Composition of different hardfacing alloys

Parameters search for Tribaloy 700

Thick hardfacing coatings are obtained mainly by a fusion process if full density and metallurgical bounding are required as in our case. Among them, the Plasma Transferred Arc Welding (PTAW) is mostly used, qualified and considered as the nominal process for this type of applications.

However, compared to conventional fusion processes, laser cladding can provide interesting properties: the dilution of substrate can be accurately controlled and reduced, high solidification speed and thermal gradient can give a very fine microstructure with homogeneous properties and higher hardness (ref. K. Komvopoulos (1990) [14]). Therefore, even if the PTAW is still used and investigated in the project, we have decided to propose to deposit the selected materials by laser cladding as an alternative process that could improve the material properties. Previous results on laser cladding of Stellite 6 and Colmonoy 52 have been presented in [10]. Now, we present the recent experiments and analysis achieved on Tribaloy 700.

Experimental setup

The laser cladding process has a large number of parameters that can influence on the quality of the clad tracks. It involves a lot of parameters. Among them, three main parameters are the speed processing, the powder feeding rate, the laser power.

The experimental setup is shown in the figure 2. In this project, a continuous 10kW Trumpf Disk laser was used to make deposits.

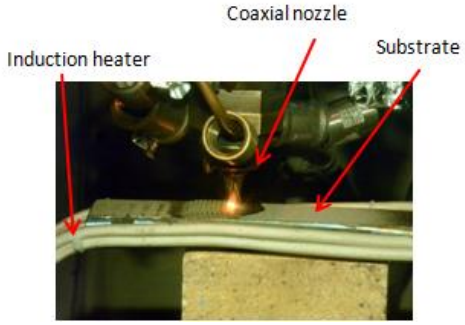

Figure 2: Laser cladding setup. View during cladding

The laser beam is at the center of the cladding nozzle. The metal powder is added by the tubes visible in figure 2. They are transported by a gas stream and injected into the melt pool. On the way through the laser beam, they absorb laser energy. The argon inert gas protection surrounding the melt pool was used to avoid oxidation. The substrate was preheated by induction. The inductor, visible in figure 2, has been designed to surround the sample and create a very homogeneous heating of the substrate. The temperature used is between 200°C and 550°C. The temperature is monitored by a pyrometer and a closed loop on the induction system. A precision of about better than+/-20°C can be obtained

Parameter search

For the experiments, specimens of 316L steel (50x50x10 mm and 200x50x20 mm) were used as substrates. Tribaloy 700 is deposited by two different processes: laser Cladding and PTAW, and their properties will be compared.

For this campaign of the parametric search, the initial parameters were selected to produce thin deposits. Their thickness is about 1.5 mm (see figure 3). The parameter window has been chosen large enough in order to evaluate the influence of the preheating :

- Laser Power : 600 to 2000W;
- Deposition speed : 400-1000mm/mn;
- Powder flow : 5-40g/mn

The laser spot size onto the substrate has been tuned by defocusing the focal spot in order to generate an acceptable melt pool geometry (typical aspect ratio height/width~2/5-2/3)

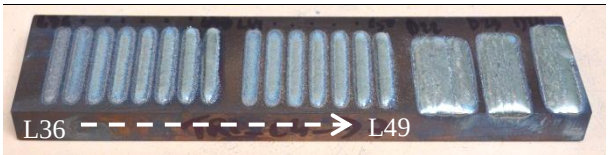

Figure 3: Examples of single track and overlaps

During the parameter search step, different causes of defects are considered. They are presented in the following section.

Porosity

The powder grain distribution is a standard one 45-150µm. The tribaloy 700 powder used for the experiments presents a very low number of porosities in the grains (see figure 5). This depends on the method of powder production. Moreover, we can see on figure 4 (right) a micrography of a grain showing a fine Laves phase structure due to rapid solidification.

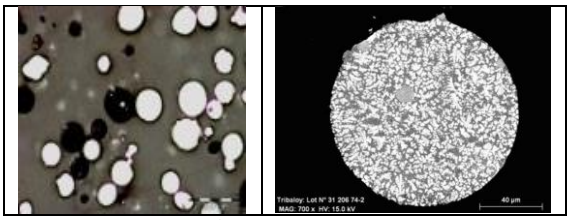

Figure 4: Micrography of the Tribaloy 700 powder selected in the study (left: global view, right: view of a grain)

As it is often seen, decreasing the size of the melt pool tends to increase the number of porosities of the clad. In our case, the number of porosity is very low thanks to the quality of the powder and a good tuning of the process parameters (adapted size and good stability of the hydrodynamics of the melt pool).

Crack and deformation

In the initial trials, the produced clads exhibit cracks. After analysis, it is clear that these cracks are not coming from hot cracking causes but certainly from stress produced during the clad. In order to avoid this, it has been considered to preheat the substrate between 500°C-600°C (see figure 5). and cooling the substrate with low cooling rate after the cladding process.

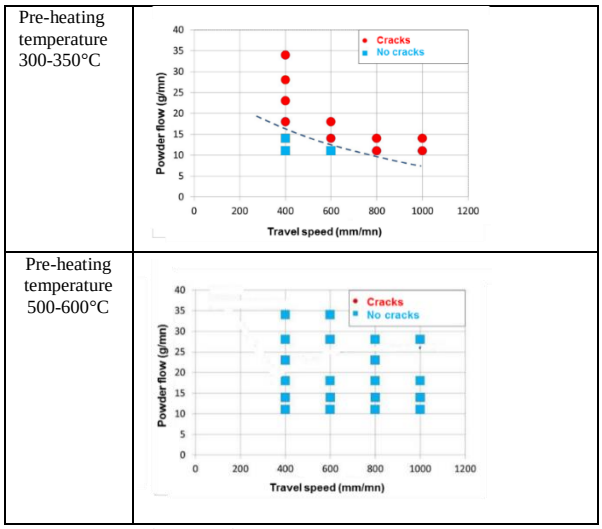

Figure 5: Influence of the pre-heating temperature on the crack susceptibility on Tribaloy 700 powder flow rate function (g/mn) of the travel speed (mm/mn))

Another way to artificially decrease the stress has been to introduce an initial opposite stress by making fusion lines at the back side of the substrate for cladding.

Finally, among the sound deposits (no cracks, few porosities and low dilution), two different tribaloy 700 samples have been selected for wear evaluation. The extreme values of travel speed have been retained providing extreme solidification speeds in our set of samples :

- one sample at 400mm/min: Tribaloy-C1,
- one sample at 1000mm/min : Tibaloy-C2.

Dilution

At low travel speed (80-150mm/min) and low powder flow rate (2-5g/min), the dilution is important and the transition between the substrate and the clad is quite smooth. The iron content goes from about 10% to the 316L iron content in about 1mm. When increasing travel speed to 200-500mm/min to1m/min), the dilution is decreased. The iron content in the clad slightly decreases about 2% instead of 3.8% in the powder. Moreover the dilution zone is reduced to less than 200µm. In the samples made by laser cladding, the interface shows a good metallurgical bounding and continuity without defect, figure 6.

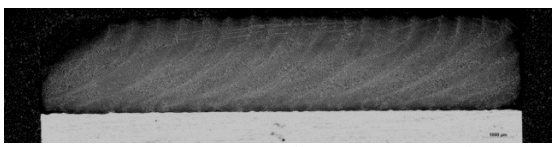

Figure 6: Optical micrography of a vertical section of a typical laser clad of tribaloy700

The transition zone is between 50 and 100µm thickness (see figure 7 (a)). For the PTAW sample, the transition zone is about 900µm thick (figure 7 (b)), showing a high dilution and leading to a high level iron content in the deposit.

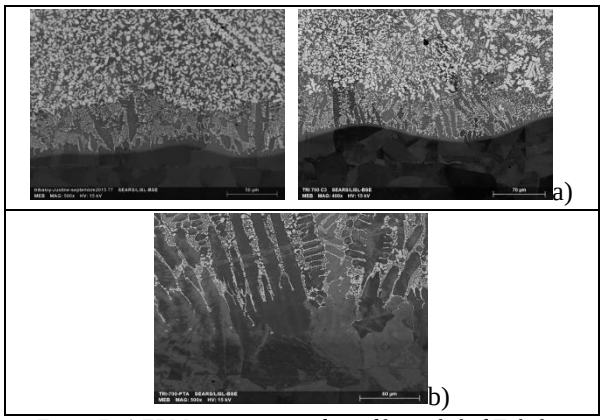

Figure 7: a) EBM images at interface of laser clad of Tribaloy 700 (Right: C1 and left: C2),x500 b) EBM images of Tribaloy700 deposited by PTAW x500

Microstructural analysis

The microstructure and chemical composition of the cladding layers have been examined by SEM and EDS. They play a crucial role for determining the properties of a component. In this study, different zones (top surface, cross section) were observed in detail to study the morphology of layers and the chemical composition.

Microstructure of the Tribaloy 700 coating consists of Nickel-based matrix (NiCrMoSiFe) and two intermetallic phases (see figure 8). The EDX results show that the difference of these intermetallic precipitates are very slight.

The cladding process presents a finer solidification microstructure (for example, size and distribution of the precipitates) than the solidification microstructure of the PTAW sample. Between both microstructure from laser process, the finest microstructure is subtracted at high deposition speed (Tribaloy-C2).

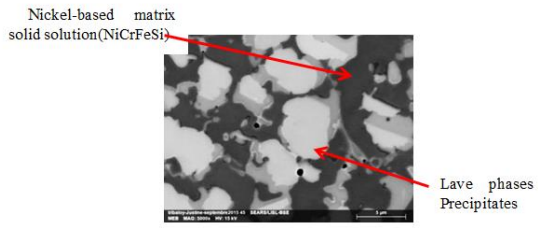

Figure 8: EBM images of a laser clad of Tribaloy 700 (X5000)

The figure 9 presents micrographies of Tribaloy 700 in the middle of the interface, respectively, by laser cladding (figure 9a) and PTAW (figure 9b).

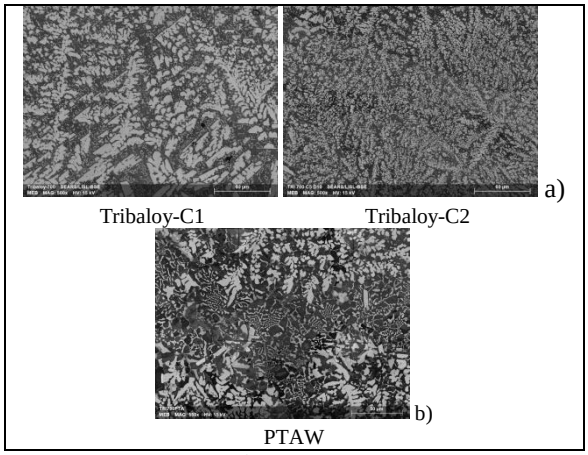

Figure 9: EBM images of Tribaloy 700 X500. a) laser cladding, b) PTAW

The figure 10 presents the micrographies (laser cladding and PTAW) of the microstructure of tribaloy 700 in the upper part of the samples

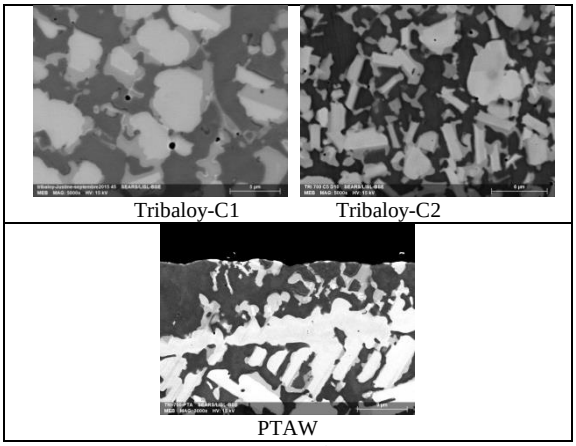

Figure 10: EBM images of Tribaloy 700

As it can been seen on table 2 related to EDX analysis of each region of image figure 8, Laves precipitate are still subject to discuss because the EDX analysis shows a mix composition of the precipitate that cannot be clearly identified to intermetallic phases, as laves phases. We observed the same intermetallic phases on the laser sample and the PTAW sample. The main difference between both is the high iron content in the PTAW sample. The iron content goes from about 25-30%W to the 316L iron content in about 1,5mm, and decreases about 4-5%W to the surface of the coating.

The study is ongoing with deeper investigation by other analysis methods as TEM or nano-Auger.

Element	Matrix phase (%w)	Laves phase (white zone) (%w)	Intermediate zone (grey zone) (%w)
Ni	60.8	33	39.6
Mo	15.1	50.40	43.7
Cr	19.6	12.00	10.4
Si	1.6	3.80	5.9
Fe	1.9	0.9	0.8
Total	99	100.2	100.4

Table 2: EDX analysis of regions presented in Figure 8

Concerning the different precipitates, the identification is ongoing. However, two main kind of hard phases can be found.

Hardness

The micro-hardness distribution accross the weld clad mapping is shows in the figure 11; In PTAW specimen, the micro-hardness dropped slight from the substrate (160 HV0.3) to the first deposit layer (410 HV0.3) overloaded with iron then we observed a second evolution after about 1500µm to the second layer (510 HV0.3). The sudden variation between first and second layer is linked to the high dilution of hard deposited material with the austenitic steel substrate

In the bounding layer, laser samples have a sudden hardness transition from 160 to 620 HB 0.3. this abrupt transition is due to the low dilution rate in laser cladding.

The level of hardness in layer deposited by PTAW is lower than laser deposited. However it is more dispersive than laser . The laser sample hardness is very homogenous.

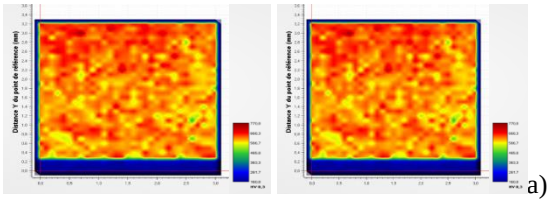
a)

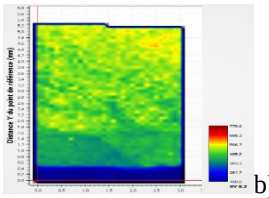
b)

Figure 11 : a)2D Vickers Micro-hardness mapping on section of a) laser cladding. Tribaloy-C1 (left) and C2 (right). b): Tribaloy PTAW

After the metallurgical analysis, we have made some tribological test that are presented in the last section.

Modelling and simulation

In parallel to the experiments, a study on modelling of laser cladding has been undertaken. The objective is clearly to, in the future, be able to simulate different experimental conditions and get a global overview of the tendencies and define more quickly the process parameters map. Thus, the simulation could be seen as complementary to experiments. The initial goal is to model and simulate the global geometry of the clads (thickness, width of tracks, information on dilution,...). Later on, it is planned to introduce microstructural model.

The numerical simulation of laser processing, in general, can be very useful for different reasons. Firstly, as the laser allows a deposition of a well-known energy distribution, the basic simulations of laser applications (only heat transfers for example) are quite easy and reasonably accurate and these simulations can be used to design experiments (power, velocity …). Secondly, a more complex kind of simulation, called multiphysics, can be developed to check the knowledge of a process and to evaluate the effect of different phenomena. For instance, it is possible and easy to erase a specific phenomenon in order to observe its effect.

In case of laser coating process, the objectives of simulation are at the same time for the process mastering and for the understanding. Indeed, the final result of the present work is the simulation of the metallurgical phases obtained after processing (not presented here). The simulation described in this paper is the first step of a larger numerical work and concerns only the computation of heat transfers with fluid flows and input material.

As the coating process is nothing but a laser metal deposition process, the model presented here is largely based on this literature.

The assumptions used to build this simulation are:

- The gas and the powder are not directly simulated.
- The metal, solid, and liquid, has no density variation (the thermal expansion is neglected).
- The fluid has a Newtonian behaviour.
- The free boundary is taken into account by the arbitrary Lagrangian Eulerian method.

The solved equations are quite classical in this kind of simulation. Indeed, for the moment, only the thermal and velocity fields, in a three dimensional coordinate system are needed. Thus, the solved

equations are the heat equation *(1)*, the Navier-Stokes equation *(2)* and the mass conservation *(3)*.

$$\rho c_p^{eq} \frac{\partial T}{\partial t} + \rho c_p \vec{u}.\vec{\nabla}T = \vec{\nabla}.(\lambda \vec{\nabla}T) \quad \textbf{(1)}$$

$$\rho \frac{\partial \vec{u}}{\partial t} + \rho(\vec{u}.\vec{\nabla})\vec{u} = \vec{\nabla}.\left[-pI + \mu\left(\vec{\nabla}\vec{u} + (\vec{\nabla}\vec{u})^T\right)\right] + \rho\vec{g} \quad \textbf{(2)}$$

$$\vec{\nabla}.(\rho\vec{u}) = 0 \quad \textbf{(3)}$$

The heat equation is solved considering a Gaussian laser input and convective and radiatives losses. The "equivalent" specific heat shown in *(1)* is an efficient way to consider the latent heat of fusion.

For the fluid flow problem, the motion source is mainly the natural convection taken into account by the Boussinessq's approximation and the Marangoni's effect caused by surface tension variation. The surface tension and its variation are introduced in the model using the Laplace's law. The free boundary simulation is made using the numerical technique called ALE for Arbitrary Lagrangian Eulerian method. This method is based on a calculation of the boundary location by a Lagrangian formulation (mesh linked to the material) and on the calculation of the bulk velocity field by an Eulerian formulation (the flow travels through the grid). The mesh motion on the bulk is thus calculated arbitrary in order to enhance the mesh quality.

As this method is not conservative in terms of mass, the added material can be introduced through an imposed normal velocity. This velocity can be calculated easily because the powder input is known and the passing surface also (the fusion zone).

The obtained results are the thermal field, the velocity field and the shape of the track. (figure 12).

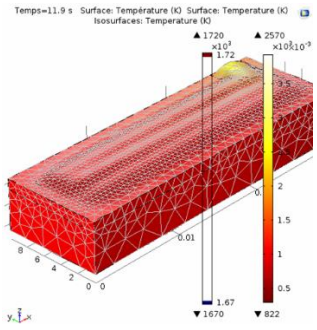

Figure 12: Results in terms of thermal field and material deposition.

This simulation is able to predict the metal deposition thickness, its width or the dilution between the substrate and the fused powder. In case of extreme application this last result can be very interesting in order to design the process parameters. This model is also built to compute the thermal field coupled to the fluid flow. This is particularly interesting for the future works concerning the calculation of specific metallurgical phases.

Tribology analysis for Tribaloy 700

The tribology analysis is an ongoing study for a large number of materials. In this section, we present new results on tribology behavior of Tribaloy 700 alloy in relation to the process parameters. Tribology tests on other materials can be found in [12].

The tribological tests were conducted on the Tribaloy-C2 and Tribaloy-C1 (fixed specimens) deposed on 316LN steel substrat using a self-made reciprocating tribometer as shown in figure 13. 316LN steel pin with 5mm diameter corresponding to the moving specimens was used as a friction pair. Applied contact stress was 31 MPa. The sliding speed and stroke were performed at 1 $mm.s^{-1}$ and 50 mm respectively at temperature of 200°C and in argon. The test duration was 10000 s, resulting in a total sliding distance of 10m. The tangential forces were recording during all test duration and are measured using four deformation gauge cells. Mass loss of the worn specimen (moving and fixed) was measured by an analytical balance (accuracy of 0.1mg). Surface morphology of specimens was researched by a three-dimensional white light interferometer, WYKO 3300 NT and a scanning electron microscope (SEM). Chemical composition of specimen was analyzed by electronic dispersive spectroscope (EDS). Microhardness was measured at a fixed load of 100g and dwell time of 15 seconds.

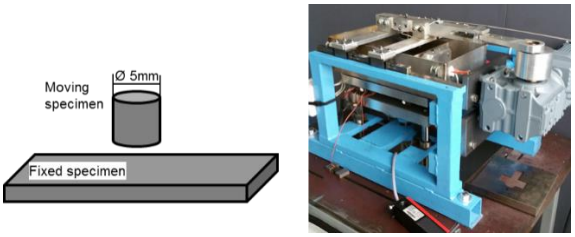

Figure 13: (a) Geometry of sliding wear test and (b) photo of tribometer.

The friction coefficient varying with time is presented in figure 14. All friction coefficients have an increase phase in the start stage of sliding but then each coating haS a different trend. Tribaloy-C1 reaches a constant value of 0.65 whereas Tribaloy-C2

decreases from 0.65 to 0.4 during all test duration. Analysis of worn track (figure 14) shows that for the Tribaloy-C2 important quantity of softer material (in this case: the pin) were adhered on the surface (positive wear depth) unlike to the profile of the Tribaloy-C1 which presents some shallow groove and very small adhered material. This adhered material on the Tribaloy-C2 surface could explain the decrease of friction of coefficient during test duration. The weight losses of pin and Tribaloy confirm this result (Figure 15).

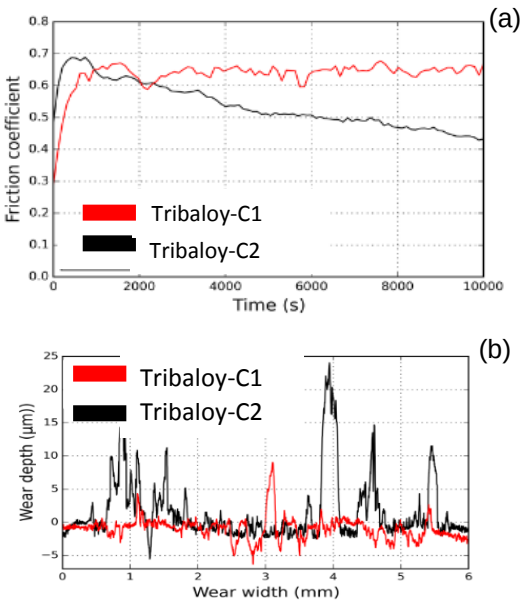

Figure 14 : (a) Friction coefficient and (b) worn track of tribaloy coating

Indeed, the weight losses of pin used with Tribaloy-C2 is very important (34 mg) whereas for the one used with Tribaloy-C1 it is low (10mg). For the coating, the weight loss is very low: for Tribaloy-C2 null and for Tribaloy-C1 2 mg.

Post mortem Vickers micro-hardness measurements of 100 g have been carried out on cross-section of the Tribaloy samples after mirror polishing. Microhardness plots for Tribaloy-C1 and Tribaloy-C2 are given in figure 16. Tribaloy-C2 shows higher microhardness than Tribaloy-C1. A gradient of hardness is clearly observed close to sliding surface (from 0 to 300µm). Tribaloy-C2 reaches a maximum value of 770 $HV_{0.1}$ whereas tribaloy-C1 reach 715 $HV_{0.1}$. This hardness gradient means that tribaloy coating undergoes work-hardening during friction test.

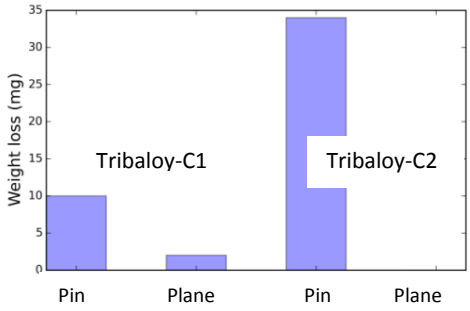

Figure 15: Weight losses of the pin and Tribaloy

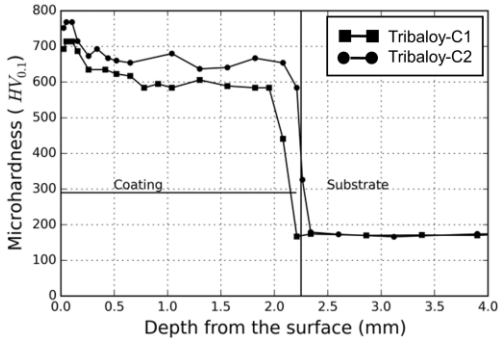

Figure 16: Microhardness profiles as a function of distance from the surface

Worn surfaces morphologies and EDS analysis after friction tests for different tribaloy alloy are presented in figures 17 and 18. It is clearly evident that all of them have a common morphology of adhesive wear generating a third body. However mechanism of adhesive wear of Tribaloy alloy was not similar. Tribaloy-C1 shows tongue-shape adhesive attachments (positive wear depth figure 14b).

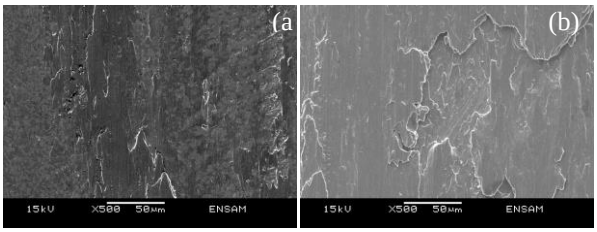

Figure 17: SEM photograph of worn surface of (a) tribaloy-C1 and (b) tribaloy-C2.

Third body was plastically deformed into tongue shape due to further sliding of mating surfaces: shearing of third body. The EDS analysis (figure 18 a-c) reveals high quantity of iron (white point of fig 15 b) and a very low quantity of nickel (dark zone of fig 15c) which indicates a material transfer from pin. There is also material detachment from the clad layer.

Tribaloy-C2 presents adhesive wear where third body is spreading. The EDS analysis (figure 18 d-f) reveals

high quantity of iron and very low quantity of nickel. This third body is principally transferred from pin. All surfaces are recovered by material transferred from pin. The spreading of this body leads to growth of the layer until reaching a limit thickness and the debonding of the third body layer.

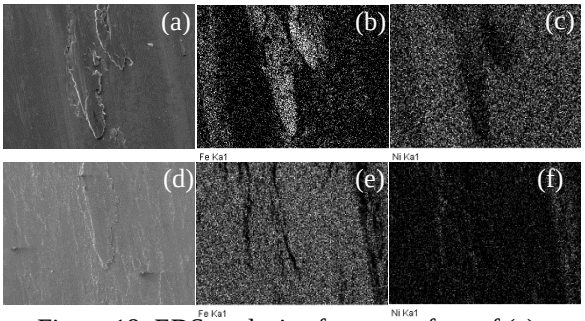

Figure 18: EDS analysis of worn surface of (a) tribaloy-C1 and (d) tribaloy-C2.

SEM micrographs of pin used as a friction pair are presented in figure 19. Pin used with tribaloy-C1 shows morphology consisting of wear grooves and severe plastically deformed adhesive attachments. EDS analysis of this pair of friction material presented in figure 20a shows that adhesive particles is composed of a mixture of the two materials : Fe, Ni and Mo are far from the composition of the pin (66% of Fe, 12% of Ni and 2.3% Mo). Both pin and tribaloy-C1 have particle detachments resulting in mixed composition of the third body. This third body could be spread onto both surfaces acting as lubricants resulting in a constant value of friction as presented in figure 14a.

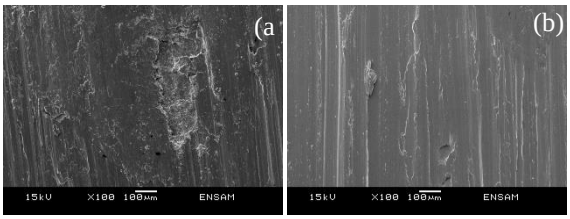

Figure 19: SEM photograph of worn surface of pin used with (a) tribaloy-C1 and (b) tribaloy-C2.

Pin used with tribaloy-C2 shows grooves in the sliding direction corresponding to an abrasive wear. EDS analysis of pin wear surface presented in figure 20b has a similar chemical composition than material of pin. There is no transfer from tribaloy-C2 to pin but only from pin to tribaloy-C2 confirming high value of wear loss of pin and the zero mass loss of tribaloy-C2 (figure 15). Particles transferred from pin material are spread on tribaloy-C2 surface resulting in a decrease of friction during the test duration (figure 14a).

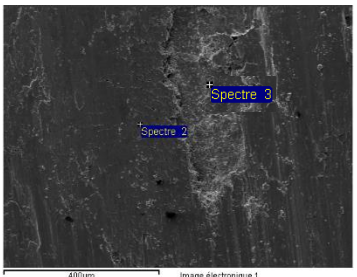

	Weight %			
Spectrum	Cr	Fe	Ni	Mo
1	16.31	39.93	27.31	16.45
2	16.02	20.99	36.62	26.36

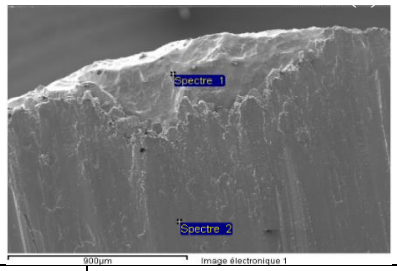

	Weight %			
Spectrum	Cr	Fe	Ni	Mo
1	17.81	70.43	9.05	0.72
2	18.09	65.18	13.08	2.65

Figure 20: EDS analysis of worn surface of pin used with (a) tribaloy-C1 and (b) tribaloy-C2.

It is clear that the variation of the microstructure from C1 to C2 has a significant influence on the wear tests. As it can be seen, the hardnesses of the two samples have a difference of about 50HV. This could partly explain the difference of wear between the two samples. However, the microstructure refinement of the precipitates can also act not only on hardness point of view, but on other micro-mechanical effects. This is still under investigation with additional analysis, as nanoindentation.

Conclusion

In this article, we have presented a new study concerning the Cobalt based hardfacing materials for Sodium Reactors. Some nickel based alloys have been selected. The laser cladding process is used for cladding the alloy onto the substrate (316L).

The parameter search has been presented for Tribaloy 700 alloy. We have demonstrated that this alloy can be deposited and that sound clads (no crack, few porosities) can be obtained.

The metallurgical analysis has been initiated and first results exhibit a thin microstructure globally equiaxed, with a good homogeneity from the interface to the substrate up to the top of the clad. Hardening phases (Laves phase type) are uniformly dispersed into the material. Some questions are under study as the nature of the phases, particularly for Laves phase like structure. This is still under investigation.

Concerning modelling and simulation, a first model has been implemented. At present, it is used for estimating the geometry of the clad. Extended comparisons of simulations to experiments will be made soon. The next step will be to integrate a metallurgical model related to the material for estimating microstructural data (size of the precipitates, distribution, constitution...)

The wear tests made on two laser cladding samples made with two different travel speed exhibit quite different wear mechanisms. This demonstrates the capability of the laser cladding process to adapt the quality of the hardfacing material to the needs by a variation of the process parameters.

Of course, corrosion test under sodium and tribo-corrosion tests under sodium at high temperature are required for making a final comparison and validation of the materials. For this, dedicated devices have to be designed and implemented. This work is not achieved yet and, thus, the tests under sodium will be made later on.

References

[1] P.M. Dunckley, T.F.J. Quinn, and J. Salter, Studies of the Unlubricated Wear of a Commercial Cobalt-base Alloy at Temperatures up to about 400°C, ASLE Transactions, 19(3), (1976), pp. 221-231

[2] H. So, C.T. Chen, and Y.A. Chen, Wear Behaviours of Laser-clad Stellite Alloy 6, Wear, 192(1-2), (1996), p. 78-84

[3] J.T.M de Hosson, and L. de Mol van Otterloo, Surface Engineering with Lasers of Co-base Materials, Surface Treatment, Computer Methods and Experimental Measurements. Comput. Mech. Publications, Southampton, UK, (1997), pp. 341-59

[4] de Mol van Otterloo, J.L. and J.T.M. de Hosson, Microstructure and abrasive wear of cobalt-based laser coatings, Scripta Materialia, 36(2), (1997), pp. 239-45

[5] D.H.E. Persson, S. Jacobson, S. Hogmark, Effect of temperature on friction and galling of laser processed Norem 02 and Stellite 21, Wear 255, (2003), pp.498–503

[6] D. H. E. Persson, Laser processed low friction surfaces, Dissertation for the degree of Licentiate of Philosophy in Materials, Materials Science Division, the Ångström Laboratory, Uppsala University, Sweden, March (2003)

[7] C. B. Bahn, B. C. Han, J. S. Bum, I. S. Hwang, Chan Bock Lee, Wear performance and activity reduction effect of Co free valves, in PWR environment, Nuclear Engineering and Design 231, (2004), pp. 51–65

[8] M. Corchia, P. Delogu, & F. Nenci,. Microstructural Aspects Of Wear-Resistant Stellite And Colmonoy Coatings by Laser Processing, *Wear*, Volume 119, (1987), pp. 137-152

[9] Kashani, A. Amadeh, & H. Ghasemi, Room and high temperature wear behaviors of nickel and cobalt base weld overlay coatings on hot forging dies. *Wear*, 262(7-8), (2007), pp. 800-806,

[10] Qian Ming, L.C. Lim, Z.D. Chen, Laser cladding of nickel-based hardfacing alloys, Surface and Coatings Technology 106, (1998), pp. 174–182

[11] D. Kesavan, & M. Kamaraj, The Microstructure and High Temperature Wear Performance of a Nickel Base Hardfaced Coating, *Surface and Coatings Technology*, 204(24), (2010), pp. 4034-4043

[12] V.D. Tran, P. Aubry, C. Blanc, J. Varlet, T. Malot, Laser Cladding And Tribocorrosion Testing Of Cobalt-Free Hardfacing Coatings For Fast Neutron Reactor, Proc. Of ICALEO 2014, (2014), paper #203

[13] C. Navas, R. Colaço, J. Damborenea, & R. Vilar, Abrasive Wear Behaviour of Laser Clad and Flame Sprayed-Melted NiCrBSi Coatings, *Surface and Coatings Technology*, 200(24), (2006), pp. 6854-6862,

[14] K. Komvopoulos, K. Nagarathnam, Processing and Characterization of Laser-Cladded Coating Materals, J. of Engineering Materials and Technology, vol. 112, (1990), pp. 131-143

Meet the Author(s)

Dr Pascal J. Aubry is Senior Expert in Laser Processing at Atomic Energy Commission (CEA) His research activities are mainly related to laser processing, additive manufacturing, surface treatment and process control.

Email: pascal.aubry@cea.fr